Superheavy Elements with the Berkeley Gas-Filled Separator

K.E. Gregorich* and V. Ninov

Lawrence Berkeley National Laboratory, MS-88, Berkeley, CA 94720, USA

Received: October 13, 1999

In April and May of 1999 the Berkeley Gas-filled Separator was used to search for the production and decay of element 118 from the ^{86}Kr + ^{208}Pb reaction, according to Smolañczuk's predictions of relatively large production rates. Three decay chains, each consisting of an implanted heavy ion, followed by a rapid (ms) succession of high-energy (> 10 MeV) alpha-particle decays were detected. These chains are consistent with the production and decay of element 118 with mass number 293. These results a) show experimental evidence for the existence of shell-stabilized superheavy elements, b) provide experimental values for refinement of nuclear mass models in the superheavy element region, and, most importantly, c) present a "new" reaction pathway for the production of superheavy elements.

In the early 1970s, the heaviest known isotopes had proton and neutron numbers near Z~106 and N~158. The experimental trends in nuclear stability indicated that with increasing Z and N, spontaneous fission (SF) would dominate the decay, resulting in ever-decreasing half-lives. However, according to the superheavy element (SHE) predictions,[1] closed proton and neutron shells near Z=114 and N=184 should result in increased stability.

Traditionally, the best nuclear reactions for production of SHE at particle accelerators were thought to involve ^{48}Ca projectiles with actinide targets, and several attempts to produce SHE were made[2] which ultimately proved unsuccessful. Recent very exciting results from experiments with ^{48}Ca projectiles and ^{238}U, ^{242}Pu, and ^{244}Pu targets have recently been reported,[3] with indications that element 114 isotopes may have been produced in the ^{48}Ca bombardments of Pu targets.

Heavy element production rates in experiments[4] to synthesize elements 110–112 indicate that it will be difficult to produce elements beyond Z=113 by the "cold fusion" approach[5] of bombarding Pb or Bi target nuclei to produce heavy compound nuclei at low excitation energies. Standard extrapolations of these production cross sections indicate that large increases in beam currents will be needed to approach production rates of one atom per month.

However, the recent predictions of Smolañczuk[6] indicate that the cold fusion of projectiles near ^{86}Kr with ^{208}Pb or ^{209}Bi targets should lead to relatively large SHE production rates. According to his calculations, the ^{208}Pb (^{86}Kr, 1n)^{293}118 reaction should proceed with a cross section of 670 pb. In addition, Smolañczuk predicted that these SHE isotopes would decay by a rapid series of high-energy α-particles. The predicted decay properties of ^{293}118 and the resulting daughter activities are presented in Table 1.

TABLE 1: Predicted[6] Decay Sequence from ^{293}118

$^{A}Z_{N}$	Q_α(MeV)	$T_{1/2}$
$^{293}118_{175}$	12.23	31 μs – 310 μs
$^{289}116_{173}$	11.37	960 μs – 9.6 ms
$^{285}114_{171}$	11.18	800 μs – 8.0 ms
$^{281}112_{169}$	11.00	610 μs – 6.1 ms
$^{277}110_{167}$	10.77	620 μs – 6.2 ms
$^{273}108_{165}$	9.69	120 ms – 1.2 s
$^{269}Sg_{163}$	8.35	8.0 min – 80 min
$^{265}Rf_{161}$	SF	41 min

*Corresponding author. E-mail: KEGregorich@lbl.gov. FAX: +1-510-486-7983.

Based on these predictions, we searched for SHE production in the interaction of ^{86}Kr projectiles with ^{208}Pb targets using the recently completed Berkeley Gas-filled Separator[7] (BGS) at the 88-Inch Cyclotron of the Lawrence Berkeley National Laboratory (LBNL). Results from these first experiments have been published.[8] A schematic of the BGS is presented in Figure 1. The $^{86}Kr^{19+}$ beam was produced in the Advanced Electron Cyclotron Resonance Source[9] and accelerated by the 88-Inch Cyclotron to an energy of 459 MeV (ΔE = 2.3 MeV FWHM). During the experiments, the beam current averaged 0.3 particle microAmperes (2.0×10^{12} ions/s). At the BGS, the beam first passed through a 0.1 mg/cm^2 carbon vacuum window before entering the 1.0 torr He gas filling the BGS. The Kr beam then passed through the ^{208}Pb targets mounted at the periphery of a 14-inch diameter rotating wheel positioned 0.5 cm downstream of the vacuum window. The targets consisted of 300–400 μg/cm^2 ^{208}Pb metal evaporated onto the downstream side of 40 μg/cm^2 carbon foils. The Pb layer was covered by an additional 10 μg/cm^2 layer of carbon to prevent sputtering of the ^{208}Pb and to aid in the blackbody radiation cooling of the targets. The ^{86}Kr energy at the center of the ^{208}Pb target material was 449 MeV.[10] The compound nucleus evaporation residues (EVRs) recoiled out of the target at near the beam momentum (EEVR = 131 MeV). Upon passing through the He gas, the EVRs experience many charge-changing collisions, leading to a well-defined average charge state. This average charge state is nearly proportional to the EVR velocity, resulting in large a large charge and velocity acceptance in the BGS. The EVRs then passed through a vertically-focusing quadrupole magnet, a 25° dipole magnet with a strong horizontally focusing field gradient, and a 45° flat-field

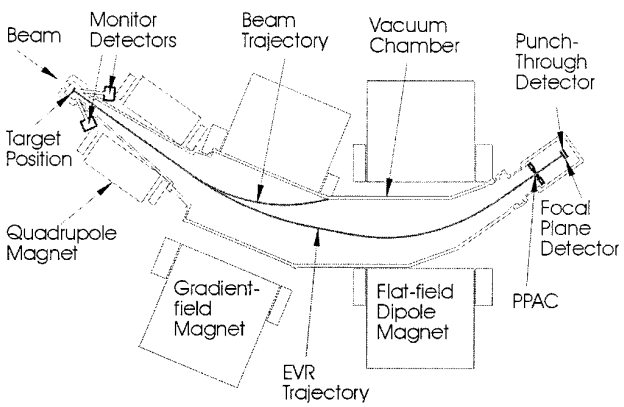

Figure 1. Schematic of the Berkeley Gas-filled Separator.

dipole magnet before entering the detector chamber. Other nuclear reaction products, unreacted beam, and scattered beam particles take on a lower magnet rigidity in the He gas, and are directed toward the beamstop along the upper edge of the vacuum chamber shown in Figure 1. The efficiency of the BGS for focusing element 118 EVRs onto the focal plane detector was estimated by measuring the α-decay of Po EVRs from a ^{86}Kr + ^{116}Cd test reaction, and comparing with the expected Po production rates.[11] This efficiency agrees well with Monte Carlo simulations of ion trajectories through the separator.

Upon entering the detector chamber, the EVRs passed through a parallel plate avalanche counter[12] (PPAC) where time and position were recorded. The Si-strip focal plane detector was located 30 cm downstream of the PPAC. This Si-strip detector was an 80 mm wide × 35 mm high and was divided into 16 vertical strips. Along each of these strips, the vertical position was measured by resistive charge division. The energy and position resolution of the Si-strip detector were determined using implanted recoil atoms from a ^{86}Kr + ^{116}Cd test reaction. The energy resolution for 5–9 MeV α particles was 30 keV FWHM, and the position resolution in the vertical direction was ± 0.58 mm. Directly behind the focal plane detector was a second Si-strip punch-through detector, used to reject particles passing through the focal plane detector. Events registering signals in both the Si-strip focal plane detector and either the PPAC or punch-through detector were interpreted as reaction products passing through the separator, while events leaving only a signal in the Si-strip detector were assumed to be decays of nuclei previously implanted in the Si-strip detector. The focal plane detector had a calculated efficiency of 60% for detection of full-energy 12-MeV α-particles from nuclei implanted to a depth of 14 μm. The other 40% of the time, α particles escape out the front of the detector, "escape alphas", depositing a partial energy ($1.5 \le E(MeV) \le 4.0$). For both the focal plane detector and the punchthrough detector, the energy, position and time of all events were recorded. The Si strip detector events were recorded over two amplifier gain settings: a low-energy setting covering 0.5–15 MeV, and a high-energy setting covering energies up to 200 MeV.

Two separate ^{86}Kr + ^{208}Pb experiments were carried out. In the first experiment, the overall rate of events registering greater than 0.5 MeV in the focal plane detector was 50 s^{-1}. In this experiment, a 5 cm × 5 cm Si-strip detector (which did not cover the entire focal plane detector) was used as the punchthrough detector. The integrated beam flux for this experiment was 0.7×10^{18} ions. For the second experiment, with an integrated beam flux of 1.6×10^{18} ions, an 8 cm × 3.5 cm Si-strip detector was used as the punchthrough detector, providing complete coverage of the focal plane detector. Improvements to the beamstop within the BGS reduced the overall count rate in the Si-strip focal plane detector to less than 20 s^{-1}. The low-energy spectrum recorded in the focal plane detector for the entire second experiment is presented in Figure 2. Figure 2(a) contains the ungated spectrum. Figure 2(b) shows the remaining events after applying a veto based on all events recorded in the PPAC. Figure 2(c) includes the additional sensitivity of applying a veto for all events registering in the punchthrough detector. Figure 2(d) shows the spectrum of all events from Figure 2(c) with $8.1 \le E(MeV) \le 13.0$ which are correlated in position and time (within 1 s) with an implanted recoil. Note that the 3 events labeled with arrows

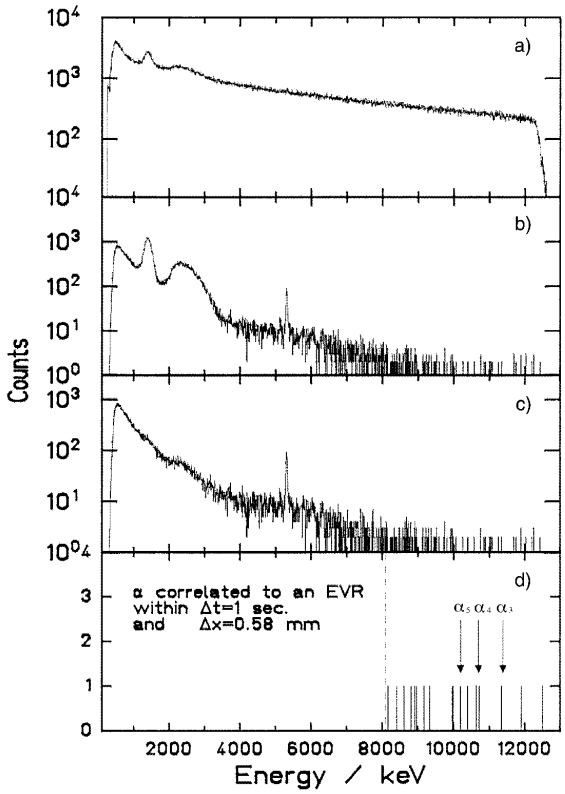

Figure 2. The low-energy spectrum in the focal plane detector for the entire second experiment. The gating conditions for the four panels are explained in the text.

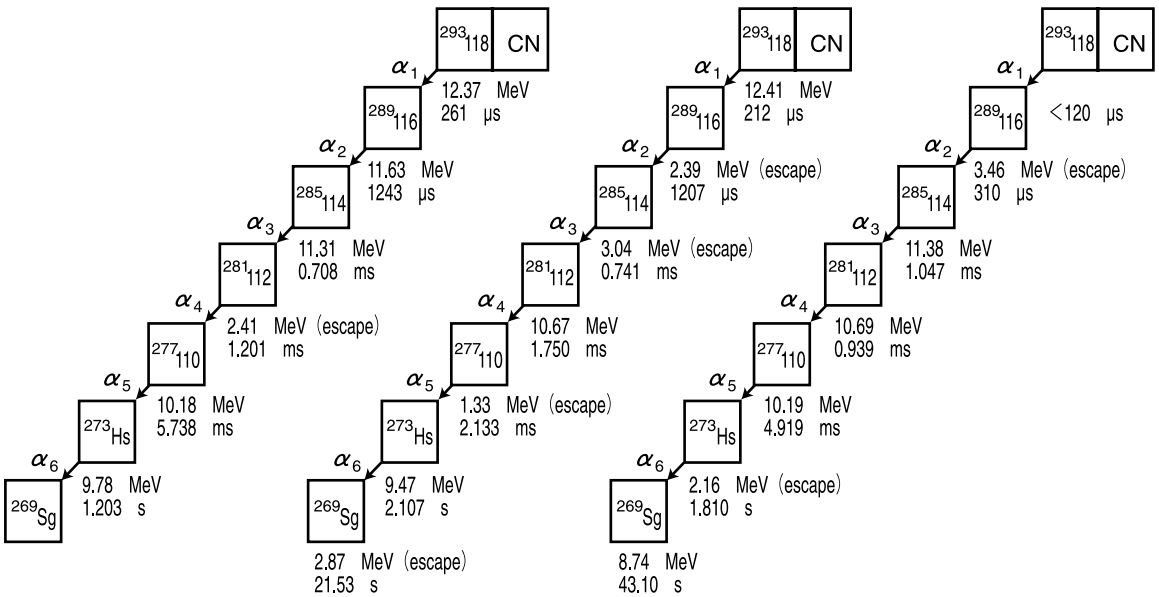

Figure 3. Observed decay chains from the reaction of 449-MeV ^{86}Kr with ^{208}Pb.

are members of a single decay chain. The detection rate for α-particles with $4.0 \le E(MeV) \le 13.0$ was 0.5 s^{-1}.

Three decay chains were observed, each consisting of an implanted heavy ion recoil (with implantation energies consistent with that expected for an element 118 recoil) correlated in position and time with chains of 6 to 7 subsequent α-particle decays. This corresponds to a production cross section of $2.2^{+2.6}_{-0.8}$ pb. The observed correlation chains are shown in Figure 3, interpreted as the decay of ^{293}118. The first two chains were observed in the first experiment, and the third was observed in the second experiment. For the third chain, we have indicated that the α-decay of the ^{293}118 was not detected because it occurred during the 120 μs dead time of the acquisition system while recording the recoil implantation event.

An analysis of the positions of the members of each chain was carried out. The FWHM position resolution for EVR-α correlations was 0.58 mm. It was assumed that the position resolution for correlations between pairs of escape alphas is the same, and for pairs of full energy α-particles it is half as large. From this, the 1-sigma position resolutions for the event types were calculated: σ_{recoil} = 0.230 mm, σ_{α} = 0.087 mm, and σ_{escape} = 0.174 mm. The weighted average and the reduced X^2 for the positions in each chain were calculated, and are presented in Figure 4. The large X^2 for the second chain results from the error in determining the positions near the bottom of the strip. (The positions were determined by comparing the pulse-heights from the top of the strips with the total pulse height. At a 3.5 mm vertical position, the signal for escape alphas measured at the top of the strip is as small as 1% of the full scale values for the amplifier and ADC.)

During the entire experiment, one additional chain was recorded, which could possibly be interpreted as being due to the implantation and decay of an atom of ^{293}118. It occurred in strip 14 during the first experiment. A recoil implantation event was recorded, followed 190 μs later by a 12.0-MeV α particle, then followed 936 μs later by a 11.4-MeV α particle, then followed at 1.125 ms, 1.740 ms, 1.503 ms, and 13.879 s later by escape alpha events, with energies of 1.3, 3.1, 2.3, and 1.2 MeV, respectively. The vertical positions (in mm) in strip 14 of the implantation, the two α events, and the four escapes were: 18.3, 18.6, 18.5, 19.1, 19.4, 19.3, and 19.8. Since strip 14 was not backed by the punchthrough detector in the first experiment, we cannot be sure of the validity of the escape alpha events. In fact, the positions of the escape events are significantly different from those for the recoil and the full energy alphas. We have therefore decided not to include this chain in any analysis of decay properties or cross section.

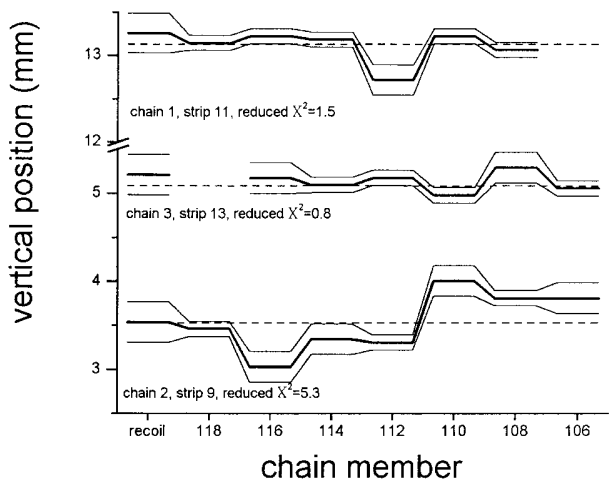

Figure 4. Analysis of the vertical positions of the three observed chains from the implantation and decay of ^{293}118. The dashed lines are the weighted average positions of the chains. The heavy lines show the measured positions of the chain members, and the thin lines indicate the 1-σ limits on the measured positions.

Based on the sequences shown in Figure 3, the half-lives of the decay chain members were calculated.[13] These half-lives are presented together with the calculated α-decay hindrance factors based on α-decay systematics for unhindered transitions[14] in Table 2, showing that the observed α-transitions have hindrance factors in the range expected for odd-N nuclei.

The observation of long decay chains of rapid, high-energy α-particles indicate the formation of SHE, as there are no know nuclei that could exhibit a similar decay pattern. The energies of the observed α-particles agree well with the predictions of Smolañcuk, supporting the proposed Z and A assignments. Statistical model considerations suggest that the ratio Γ_n/Γ_α is be proportional to $\exp\{-[S_n - (B_\alpha - Q_\alpha)]/T\}$, where S_n is the neutron separation energy, B_α is the Coulomb barrier for α emission, Q_α is the energy released in removing an α particle from the nucleus, and T is the nuclear temperature. Substituting appropriate values for the binding energies[6] and barriers[15] gives $\Gamma_n/\Gamma_\alpha \sim 60$ and similarly, $\Gamma_n/\Gamma_p \sim 200$, indicating that neutron emission is the most probable deexcitation path. Since the excitation energy of the compound nucleus is ~13 MeV,[6] emission of two particles (i.e., 2n, αn, or pn, etc.) is energetically forbidden. In addition, extrapolation of the Q_α values from known isotopes of Hs and Sg to neutron numbers at the ends of our chains indicate that deexcitation by α emission is extremely unlikely. Therefore, while other assignments are not absolutely ruled out, we are confident in the assignment of these chains to the decay of ^{293}118.

TABLE 2: Measured α-Particle Energies, Half-Lives, and Hindrance Factors[14] for Decay Chain Members

$^{A}Z_N$	E-α (MeV)	Measured $T_{1/2}$	H.F.[a]
$^{293}118_{175}$	12.39	120^{+180} μs	8.7 (4.3 – 14)
$^{289}116_{173}$	11.63	600^{+860} μs	3.6 (1.8 – 8.9)
$^{285}114_{171}$	11.34	580^{+870} μs	3.0 (1.5 – 7.4)
$^{281}112_{169}$	10.68	890^{+1300} μs	0.5 (0.2 – 1.2)
$^{277}110_{167}$	10.18	$3.0^{+4.7}$ ms	0.4 (0.2 – 1.0)
$^{273}108_{165}$	9.78	$1.2^{+1.7}$ s	110 (56 – 270)[b]
	9.47		15 (8 – 37)[b]
$^{269}Sg_{163}$	8.74	~22 s[c]	~4.2

[a] HF for the most probable half life with HF for lower and upper half-life limits in parentheses.

[b] hindrance factors assuming each α-energy has 50% abundance.

[c] half-life is approximate because maximum search time is poorly defined.

In Figure 5, we compare our measured α particle energies with predictions of several modern nuclear mass models. The best agreement with our observations is obtained with Smolañczuk's prediction. The finite range droplet model[16] and the Thomas-Fermi model[17] are macroscopic-microscopic models, which both use Möller's shell effects. It appears that their predicted Z = 114 shell effect near N = 175 is too strong. Q_α values from the SLy4 Skyrme-Hartree-Fock Bogoliubov method[18] shows extra stability near Z=116 which does not appear in the experimental data. The empirical mass model of Liran and Zeldes[19] may not be appropriate for extrapolation into this region.

We have presented evidence for the first synthesis of new superheavy elements (^{293}118 and its decay products ^{289}116, ^{285}114, ^{281}112, ^{277}110, ^{273}Hs, and ^{269}Sg). The measured α-decay energies can be used directly for refinement of mass and shell models. Our results show an unexpected viability of the cold fusion approach to the synthesis of superheavy nuclei using projectiles heavier than ^{70}Zn with targets near ^{208}Pb. The 2.2

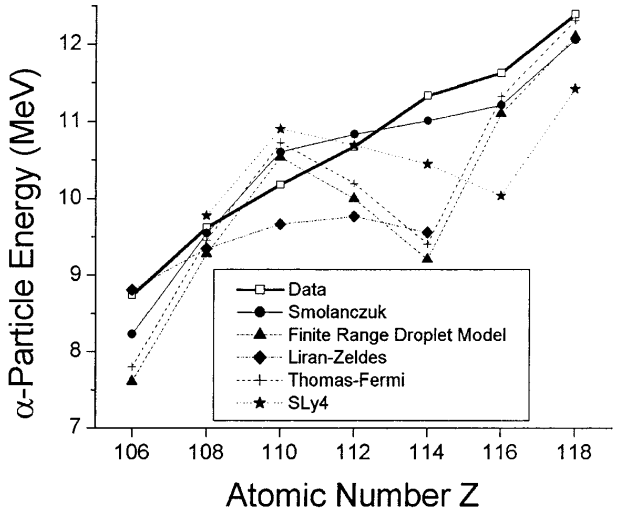

Figure 5. Comparison of the α-particle energies observed in this work with the predictions of various mass models for the N – Z = 57 nuclei.

pb cross section, while it than 300 times smaller than that predicted by Smolañczuk, is orders of magnitude larger than expected from extrapolations from cold fusion reactions with lighter projectiles.[4] This relatively large cross section may be explained by the idea of "unshielded fusion"[20] where with heavier projectiles, the optimal bombarding energy for the 1n deexcitatoin channel is above the Coulomb barrier so that the Coulomb barrier is no longer the first thing stopping the fusion process.

We gratefully acknowledge the operations staff of the 88-Inch Cyclotron for providing intense, steady beams of ^{86}Kr. We thank B. Lommel and W. Talheimer of Gesellschaft für Schwerionenforschung for providing the entrance windows and lead targets. We thank N. Kurz and H. Essel for help in setting up the data acquisition system, and G. Münzenberg and S. Hoffman for their support. We gratefully acknowledge R. Smolañczuk for helpful discussions and continuous theoretical support. We thank M. Steiner, J. Yurkon, and D.J. Morrissey at Michigan State University for lending the PPACs. Financial support was provided by the Office of High Energy and Nuclear Physics, Nuclear Physics Division and the Office of Energy Research, Office of Basic Energy Sciences, Chemical Sciences Division of the U.S. Department of Energy under Contract No., DE-AC03-76SF0098 and Grant No., DE-FG06-88ER40402.

References

(1) G. T. Seaborg and W. Loveland, *The Elements Beyond Uranium* (Wiley, New York, 1990).
(2) R. J. Otto et al., J. Inorg. Nucl. Chem. **40**, 589 (1978).
P. Armbruster et al., Phys. Rev. Lett. **54**, 406 (1985).
R. W. Lougheed, J. M. Landrum, E. K. Hulet, J. F. Wild, R. J. Dougan, A. D. Dougan, H. Gäggeler, M. Schädel, K. J. Moody, K. E. Gregorich, and G. T. Seaborg et al., Phys. Rev. C **32**, 1760 (1985).
(3) Yu. Ts. Oganessian et al., Eur. Phys. J. A **5**, 63 (1999).
Yu. Ts. Oganessian et al., Nature **400**, 242 (1999).
Yu. Ts. Oganessian et al., LLNL Preprint UCRL-JC-133388 (1999) (submitted to Phys. Rev. Lett.).
(4) A. Ghiorso et al., Phys. Rev. C **51**, R2293 (1995).
S. Hoffman, Rep. Prog. Phys. **61**, 373 (1998).
Y. Lazarev et al., Phys. Rev. C **54**, 620 (1996).
(5) Yu. Ts. Oganessian et al., Nucl. Phys. **A239**, 353 (1975).
(6) R. Smolañczuk, Phys. Rev. C **59**, 2634 (1999).
R. Smolañczuk, Phys. Rev. C **60**, 021301 (1999).
R. Smolañczuk, Soltan Inst. for Nuclear Studies Preprint SINS/Th/2/1999 (submitted to Phys. Rev. Lett.).
R. Smolañczuk, Lawrence Berkeley National Lab. Preprint LBNL-44132 (submitted to Phys. Rev. Lett.).
(7) V. Ninov and K. E. Gregorich, ENAM98, edited by B. M. Sherrill, D. J. Morrissey, and C. N. Davids (AIP, Woodbury, 1999) p. 704 and http://bgsmc01.lbl.gov/.
(8) V. Ninov et al., Phys. Rev. Lett. **83**, 1104 (1999).
(9) X. Q. Xie and C. M. Lyneis, Rev. Sci. Instr. **67**, 886 (1996).
(10) F. Hubert et al., Atom. Data Nucl. Data Tables **46**, 1 (1990).
(11) W. Reisdorf, Z. Phys. A **300**, 227 (1981).
(12) D. Swan, J. Yurkon, and D. J. Morrissey, Nucl. Instr. and Meth. A **348**, 314 (1994).
(13) K. E. Gregorich, Nucl. Instr. and Meth. A **302**, 135 (1991).
(14) Y. Hatsukawa et al., Phys. Rev. C **42**, 674 (1990).
(15) W. E. Parker et al., Phys. Rev. C **44**, 774 (1991).
(16) P. Möller et al., Atom. Data Nucl. Data Tables **59**, 185 (1995).
(17) W. D. Myers and W. J. Swiatecki, Nucl. Phys. **A601**, 141 (1996).
(18) S. Cwiok et al., Phys. Rev. Lett. **83**, 1108 (1999).
(19) S. Liran and N. Zeldes, Atom. Data Nucl. Data Tables **17**, 431 (1976).
(20) W. J. Swiatecki (private communication, 1999).